Proceedings of the American Control Conference
Arlington, VA June 25-27, 2001

Adaptive Control for Z-Axis MEMS Gyroscopes[1]

Sungsu Park[2] and Roberto Horowitz[3]

Berkeley Sensor and Actuator Center
Department of Mechanical Engineering
University of California at Berkeley
Berkeley, CA 94720

Abstract

A new angular rate-sensing scheme for z-axis MEMS oscillatory gyroscopes, which is based on observer-based adaptive control, is presented. The proposed control scheme estimates the component of the angular velocity vector, which is orthogonal to the plane of oscillation of the gyroscope (z-axis), as well as compensates friction forces, and fabrication imperfections, which cause model parameter variations and the presence of off-diagonal terms in the system's stiffness and damping matrix. The convergence and resolution analysis shows that the proposed observer-based adaptive controlled scheme offer several advantages over conventional sensing strategies, including a larger operational bandwidth, producing no zero-rate output, the ability of self-calibration and a large robustness to parameter variations cause by fabrication defects and ambient conditions.

1 Introduction

Gyroscopes are commonly used sensors for measuring angular velocity in many areas of applications such as navigation, homing, and control stabilization. Although, conventional rotating wheel, fiber optic and ring laser gyroscopes have dominated a wide range of applications, they are too large and, most often too expensive to be used in many emerging applications.

Recent advances in micro-machining technology have made the design and fabrication of MEMS gyroscopes possible. These devices are several orders of magnitude smaller than conventional mechanical gyroscopes (*mm* level), and can be fabricated in large quantities by batch fabrication processes. Thus, there is great potential to significantly reduce their fabrication cost. The emergence of MEMS gyroscopes is opening up new market opportunities and applications in the area of low-cost and medium performance inertial devices, including consumer electronics, automotive applications, GPS augmentation and a wide range of new military applications.

All MEMS gyroscopes are laminar vibratory mechanical structures fabricated on polysilicon or crystal silicon. Common fabrication steps include bulk micromachining, wafer-to-wafer bonding, surface micromachining, and high aspect ratio micromachining. Each of these fabrication steps involves multiple process steps such as deposition, etching and patterning of materials. Depending on the technology used, different numbers of steps may be involved in the fabrication of a MEMS gyroscope, and different fabrication tolerances can be achieved. Therefore, small imperfections always occur during the fabrication process [1]. Fabrication imperfections that produce asymmetric structures, mis-alignment of actuation mechanism and deviations of the center of mass from the geometric center, result in undesirable, systematic perturbations in the form of mechanical and electrostatic forces, which degrade the performance of a gyroscope. As a consequence, some kind of control is essential for improving the performance and stability of MEMS gyroscopes, by effectively canceling "parasitic" effects.

Most published angular rate sensing techniques are based on the so-called open-loop mode of operation, which rely on heuristic methods for tuning unfavorable parameters [2]. Few feedback control methods have been presented in the open literatures that measure angular velocity in a closed-loop mode of operation. Recent closed-loop approaches include the use of preview control based on Kalman filtering [3], and the force-balancing feedback control [4].

This paper presents a new observer-based adaptive control scheme for MEMS gyroscopes. The proposed controller is self-calibrating, compensates for friction forces, and fabrication imperfections which normally cause quadrature error, and produces an unbiased angular velocity measurement that has no zero-rate output (ZRO).

2 Modeling of Z-Axis MEMS Gyroscope Dynamics

Common MEMS vibratory gyroscope configurations include a proof mass suspended by spring suspensions, and

[1]Research supported by DARPA under Contract N66001-97-C-8643.
[2]Post-doctoral Researcher; spark@me.berkeley.edu
[3]Professor; horowitz@me.berkeley.edu

an electrostatic actuation and sensing mechanisms for forcing an oscillatory motion and sensing the position and velocity of the proof mass. These mechanical components can be modeled as a multi-degree-of-freedom mass, spring and damper system.

To derive the gyroscope's dynamic equations of motion, two coordinate systems are introduced: the inertial frame, which is fixed in an inertial space, and the gyro frame, which is fixed to the rotation platform. Figure 1 shows a simplified model of a MEMS gyroscope having two degrees of freedom (x any y axes) in the associated Cartesian reference frames. Assume that the gyro frame $\{g\}$ is rotated with respect to inertial frame $\{e\}$ by the angular velocity

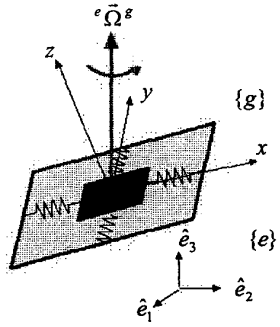

Figure 1. A model of a MEMS z-axis gyroscope

vector ${}^{e}\vec{\Omega}^{g}$, then the equation of the motion of the proof mass of the gyroscope can be derived from Newton's law.

If we wish to measure the component of the angular velocity along the z-axis, the motion of the proof mass can be constrained to be only along the x-y plane by making the spring stiffness in the z direction much larger than those in the x and y directions. Assuming that the measured angular rate is almost constant over a sufficiently long time interval and that linear accelerations are cancelled out, either as an offset from the output response or by applying counter-control forces, the equations of motion of a gyroscope are described in $\{g\}$ frame as follows.

$$\begin{aligned} m\ddot{x}+d_1\dot{x}+k_1-m(\Omega_y^2+\Omega_z^2)\,x+m\Omega_x\Omega_y y&=\tau_x+2m\Omega_z\dot{y} \\ m\ddot{y}+d_2\dot{y}+\left(k_2-m(\Omega_x^2+\Omega_z^2)\right)y+m\Omega_x\Omega_y x&=\tau_x-2m\Omega_z\dot{x} \end{aligned} \quad (1)$$

where x and y are the coordinates of the proof mass relative to the gyro frame, $d_{1,2}$, $k_{1,2}$ are damping and spring coefficients, $\Omega_{x,y,z}$ are the angular velocity components along each axis of the gyro frame and $\tau_{x,y}$ are control forces. The two last terms in equation (1), $2m\Omega_z\dot{x}$ and $2m\Omega_z\dot{y}$, are due to the Coriolis forces and are the terms which are used to measure the angular rate Ω_z. As seen in equation (1), in an ideal gyroscope, only the component of the angular rate along the z-axis, Ω_z, causes a *dynamic coupling* between the x and y axes, under the assumption that $\Omega_x^2 \approx \Omega_y^2 \approx \Omega_x\Omega_y \approx 0$. In practice, however, small fabrication imperfections always occur, and also cause dynamic coupling between the x and y axes through the asymmetric spring and damping terms. These are major factors which limit the performance of MEMS gyroscopes. Taking into account fabrication imperfections, the dynamic equations (1) are modified as follows [1].

$$\begin{aligned} m\ddot{x}+d_{xx}\dot{x}+d_{xy}\dot{y}+k_{xx}x+k_{xy}y&=\tau_x+2m\Omega_z\dot{y} \\ m\ddot{y}+d_{xy}\dot{x}+d_{yy}\dot{y}+k_{xy}x+k_{yy}y&=\tau_y-2m\Omega_z\dot{x} \end{aligned} \quad (2)$$

Equation (2) is the governing equation for a z-axis MEMS gyroscope. Fabrication imperfections contribute mainly to the asymmetric spring and damping terms, k_{xy} and d_{xy}. Therefore these terms are unknown, but can be assumed to be small. The x and y axes spring and damping terms are mostly known, but have small unknown variations from their nominal values. The proof mass can be determined very accurately. However, even if there are small-unknown variations in the proof mass, this will not be a problem, because equation (2) can be scaled by the proof mass. The components of angular rate along x and y axes are absorbed as part of the spring terms as unknown variations. Note that the spring coefficients k_{xx} and k_{yy} include the electrostatic spring softness.

Non-dimensionalizing the equations of motion of a gyroscope is useful because the numerical simulation is easy, even under the existence of large two time-scales differences in gyroscope dynamics. One time scale is defined by the resonant natural frequency of the gyroscope, $\sqrt{k_{xx}/m}$, the other by the applied angular rate Ω_z. Nondimensionalization also produces a unified mathematical formulation for a large variety of gyroscope designs. In this paper, controllers will be designed based on non-dimensional equations. The realization to a dimensional control for the specific gyroscope can be easily accomplished by multiplying the dimensionalizing parameters by the non-dimensional controller parameters. Based on m, q_0 and ω_n, which are a reference mass, length and natural resonance frequency respectively, where m is a proof mass of the gyroscope, the non-dimensionalized equation (2) can be derived as follows:

$$\begin{aligned} \ddot{x}+\omega_x/Q_x\,\dot{x}+d_{xy}\dot{y}+\omega_x^2x+\omega_{xy}y&=\tau_x+2\Omega_z\dot{y} \\ \ddot{y}+d_{xy}\dot{x}+\omega_y/Q_y\,\dot{y}+\omega_{xy}x+\omega_y^2y&=\tau_y-2\Omega_z\dot{x} \end{aligned} \quad (3)$$

where Q_x and Q_y are the x and y axis quality factor respectively. And, $\omega_x=\sqrt{k_{xx}/(m\omega_0^2)}$, $\omega_y=\sqrt{k_{yy}/(m\omega_0^2)}$, $\omega_{xy}=k_{xy}/(m\omega_0^2)$, $d_{xy}\leftarrow d_{xy}/(m\omega_0)$, $\Omega_z\leftarrow\Omega_z/\omega_0$, $\tau_x\leftarrow\tau_x/(m\omega_0^2q_0)$ and $\tau_y\leftarrow\tau_y/(m\omega_0^2q_0)$. The natural frequency of the x or y axis can be used to define the

nondimensionalizing parameter ω_0. Since the usual displacement range of the MEMS gyroscope in each axis is at a sub-micrometer level, it is reasonable to choose 1 μm as a reference length q_0. Considering that the usual natural frequency of each of the axis of a vibratory MEMS gyroscope is in the *KHz* range, while the applied angular rate may be in the degrees per second or degrees per hour range, the non-dimensional angular rate that we want to estimate is respectively in the range between 10^{-4} and 10^{-10}!

3 Review of Conventional Modes of Operation

The conventional MEMS gyroscope mode of operation reduces to driving one of the modes of the gyroscope into a known oscillatory motion and then detecting the Coriolis acceleration coupling along the sense mode of vibration, which is orthogonal to the driven mode [2]. The response of the sense mode of vibration provides information about the applied angular velocity. The conventional mode of operation is classified into the open-loop mode and the closed-loop mode. The main difference between the closed-loop and open-loop mode of operation lies in that in the former the displacement of the sense axis is controlled to zero, while in the latter it is measured.

Most MEMS gyroscopes are currently operated in the open-loop mode. The main advantage of the open-loop mode of operation is that circuitry used for the operation of gyroscope in this mode is simpler than in the other modes, since there is no control action in the sense axis. Thus, this mode can be implemented relatively easily and cheaply. However, under an open-loop mode of operation, the gyroscope's angular rate scale factor is very sensitive, and not constant over any appreciable bandwidth, to fabrication defects and environment variations. Therefore, the application areas for the open-loop mode are limited to those which require low-cost and low-performance gyroscopes.

In contrast to the open-loop mode of operation, in the closed-loop mode of operation, the sense amplitude of oscillation is continuously monitored and driven to zero. As a consequence, the bandwidth and dynamic range of the gyroscope can be greatly increased beyond what can be achieved with the open-loop mode of operation [4]. However, under conventional closed-loop mode of operation, it is difficult to ensure a constant noise performance, in the face of environment variations such as temperature changes, unless an on-line mode tuning scheme is included. Moreover, there are practical difficulties in designing a feedback controller which closed-loop system is stable and sufficiently robust, for gyroscopes with high Q (quality factor) systems. Therefore, the application areas for conventional closed-loop mode of operation are those which requires medium-cost and medium-performance (large bandwidth but limited resolution) gyroscopes.

Both the open-loop and closed-loop modes are inherently sensitive to some types of fabrication imperfections which can be modeled as cross-damping terms d_{xy}, which produce ZRO. The detrimental effect of the asymmetric damping term d_{xy} on gyroscope performance has not been considered by many researchers so far. However, its effect should not be underestimated.

With the conventional modes of operation, it is also very difficult to identify and compensate for all fabrication imperfections in an on-line fashion, due to the simple internal dynamics of the gyroscope when is operating under these modes. One solution to achieve on-line compensation of fabrication imperfections may be to create a richer gyroscope dynamics than can be achieved in the conventional modes of operation. This idea led us to investigate an adaptive algorithm for estimating the angular rate, and at the same time, identifying and compensating for fabrication imperfections in an on-line fashion, by extending gyroscope dynamics further.

4 Adaptive Mode of Operation

This section proposes a new operating strategy for MEMS gyroscopes, which will be referred to as the adaptive mode of operation. Its aim is to achieve (1) on-line compensation of fabrication imperfections, (2) closed-loop identification of the angular rate, (3) to attain a large bandwidth and dynamic range, and (4) self-calibration operation.

The proposed adaptive mode of operation will operate based on observer-based adaptive control algorithm which needs only position measurements of the proof mass of the gyroscope. Since the observer based adaptive control is the extension of the adaptive control based on velocity measurement, we first briefly derive the development of former scheme.

4.1 Velocity Measurement-based Adaptive Control

The basic idea of the adaptive control approach is to treat the angular rate, along with the effect of fabrication defects, as an unknown gyroscope parameter, which must be estimated using a parameter adaptation algorithm (PAA).

The adaptive control problems of the gyroscope is formalized as follows: given the equation with unknown constant parameters D, K and Ω,

$$\ddot{q} + D\dot{q} + Kq = \tau \quad 2\Omega\dot{q} \tag{4}$$

where

$$q = \begin{bmatrix} x \\ y \end{bmatrix} \quad \tau = \begin{bmatrix} \tau_x \\ \tau_y \end{bmatrix} \quad \Omega = \begin{bmatrix} 0 & -\Omega_z \\ \Omega_z & 0 \end{bmatrix}$$

$$D = \begin{bmatrix} d_{xx} & d_{xy} \\ d_{xy} & d_{yy} \end{bmatrix} \quad K = \begin{bmatrix} \omega_x^2 & \omega_{xy} \\ \omega_{xy} & \omega_y^2 \end{bmatrix}$$

determine the control law τ based on measuring q and $\dot{q}$, such that the dynamic range is constrained within a

specified region and Ω is estimated correctly. With this kind of problem formulation, we treat the gyroscope as a multi-dimensional dynamic device.

In a similar manner to other adaptive control problems, the persistent excitation condition is an important factor to estimate the angular rate correctly. To solve this problem, a trajectory following approach is used. The reference trajectory that the gyroscope must follow must be generated so that the persistent excitation condition is met. Suppose that a reference trajectory is generated by an ideal oscillator and that the control objective is to make trajectory of real gyroscopes follow that of the reference model. The reference model is defined as

$$\ddot{q}_m + K_m q_m = 0 \tag{5}$$

where $K_m = diag\{\omega_1^2, \omega_2^2\}$ are the reference resonant modes of both axis. We present the following two theorems, whose proofs can be found in [5].

Theorem 1

For the gyroscope dynamics (4) under the trajectory following control law (6) and adaptation laws (7), the trajectory error $e_p = q - q_m$, and its time derivative $\dot{e}_p$ and $\ddot{e}_p$ converge globally and exponentially to zero.

$$\tau = \hat{D}\dot{q}_m + \hat{R}q_m + 2\hat{\Omega}\dot{q}_m + \tau_0 \tag{6}$$

$$\begin{aligned} \dot{\hat{R}} &= \frac{1}{2}\gamma_R\left(\tau_0 q_m^T + q_m \tau_0^T\right) \\ \dot{\hat{D}} &= \frac{1}{2}\gamma_D\left(\tau_0 \dot{q}_m^T + \dot{q}_m \tau_0^T\right) \\ \dot{\hat{\Omega}} &= \gamma_\Omega\left(\tau_0 \dot{q}_m^T - \dot{q}_m \tau_0^T\right) \end{aligned} \tag{7}$$

where $R = K - K_m$, $\hat{D}$, $\hat{R}$, $\hat{\Omega}$ are estimates of D, R and Ω, $\tau_0 = -\gamma\ \dot{e}_p$, $\gamma = diag\{\gamma_1, \gamma_2\}$ and the reference signal q_m and $\dot{q}_m$ are given by (5).

Theorem 2

Using the control law (6) and adaptation laws (7), if the gyroscope is controlled to follow the mode-unmatched reference model (5), i.e. $\omega_1 \neq \omega_2$, the persistent of excitation condition is satisfied and all unknown gyroscope parameters, including the angular rate, are estimated correctly.

Theorems 1 and 2 show that the motion of a mode-unmatched gyroscope, in which the resonance frequency of the x-axis is different from that of the y-axis, has sufficient persistence of excitation to permit the identification of all major fabrication imperfections as well as "input" angular rate. This means that adaptive controlled gyroscope has no ZRO and is self-calibrating.

4.2 Velocity Observer-based Adaptive Control

The position and velocity measurements are corrupted by electrical noise in the sensing circuit. The analysis of the stochastic properties of the sensing noises, as well as the estimation of their intensity is given in literature [2], and only results are presented here. The estimated power spectral densities of the position (S_p) and velocity (S_v) measurements are given by

$$S_p = \left(\frac{2C_0 + C_p}{2V_0 \dfrac{dC}{dy}}\right)^2 4k_B T R_{wire},\ S_v = \left(V_{DC}\frac{dC}{dy}\right)^{-2}\frac{k_B T}{R_{amp}} \tag{8}$$

where k_B, C_p, C_0, R_w and T are respectively Boltzmann's constant, the device's parasite capacitance, nominal sensing capacitance, wiring resistance and absolute temperature, repectively. Both are assumed zero-mean white noises.

Current velocity sensing circuitry technology produces a noise with spectral power that is 3~4 orders of magnitude larger than the ideally expected value $S_v = \omega^2 S_p$. Thus, it is necessary to introduce an adaptive observer to avoid measuring the velocity of the proof mass directly.

In designing such a velocity observer, if we can preserve the structural property of the basic adaptive control structure, then the analytic performance results of the basic adaptive control can be easily extended for the case when velocity estimation is utilized. In order to estimate velocity, we introduce the following observer.

$$\begin{aligned} \dot{\hat{q}}_p &= \hat{q}_v + L(q - \hat{q}_p) \\ \dot{\hat{q}}_v &= -K_m \hat{q}_p \end{aligned} \tag{9}$$

where $\hat{q}_p$ is the estimate of the position, $\dot{\hat{q}}_p$ is the estimate of the velocity, and L is the observer gain. To complete the modification, the velocity term $\dot{q}$ in the adaptive control (6) and parameter adaptation laws (7) is replaced by $\dot{\hat{q}}_p$.

We present the following theorem without proof. A proof can be found in [5].

Theorem 3

Consider the gyroscope dynamics (4) under the trajectory following control (6) and adaptation laws (7), where $\tau_0 = -\gamma\ \dot{\hat{e}}_p$, $\dot{\hat{e}}_p = \dot{\hat{q}}_p - \dot{q}_m$ and $\dot{\hat{q}}_p$ is the observer (9). It is always possible to choose an observer gain L in (9) such that the trajectory estimation errors $\tilde{q}_p = \hat{q}_p - q$ and $\tilde{q}_v = \hat{q}_v - \dot{q}$, the trajectory error $e_p = q - q_m$, their time derivatives, and the parameter estimation errors converge locally, uniformly and exponentially to zero.

5 Performance Analysis

We now examine the convergence rate and stochastic variance of the angular rate estimate. This analysis gives us an estimate of the bandwidth and resolution of an adaptive controlled gyroscope.

5.1 Convergence Rate Analysis

Averaging analysis is commonly used in the adaptive literature to determine the convergence properties of the adaptation algorithm [6]. This technique is utilized to estimate the convergence rate of the gyroscope parameter estimates, including the input angular rate estimate. Since parameter estimation dynamics is slower than trajectory and trajectory estimation dynamics, we can relate the slow parameter estimation dynamics with the averaged parameter estimation dynamics. Using the facts that the products of sinusoids at different frequencies have zero average, the averaged dynamics of the parameter error estimates can be obtained. All parameter estimate error dynamics are coupled to each other. However, as the control gain $\gamma_{1,2}$ and observer gain $L_{1,2}$ become large enough and/or the reference model resonant frequencies ω_1 and ω_2 become close enough, the coupling effect of the dynamics of all parameter estimate errors is decoupled, except for the estimate error dynamics of the asymmetric damping term and angular rate. Their dynamics remain coupled and is given by

$$\begin{bmatrix} \tilde{d}_{xyav} \\ \tilde{\Omega}_{zav} \end{bmatrix} \approx \begin{bmatrix} a_{11} & a_{12} \\ a_{21} & a_{22} \end{bmatrix} \begin{bmatrix} \tilde{d}_{xyav} \\ \tilde{\Omega}_{zav} \end{bmatrix} \qquad (10)$$

where

$$a_{11} = -\frac{\gamma_D}{4}\left(X_0^2\omega_1^2 + Y_0^2\omega_2^2\right),\ a_{12} = -\frac{\gamma_D}{2}\left(X_0^2\omega_1^2 - Y_0^2\omega_2^2\right)$$

$$a_{21} = -\frac{\gamma_\Omega}{2}\left(X_0^2\omega_1^2 - Y_0^2\omega_2^2\right),\ a_{22} = -\gamma_\Omega\left(X_0^2\omega_1^2 + Y_0^2\omega_2^2\right)$$

By equation (10), if we set the reference model oscillations such that $X_0\omega_1 = Y_0\omega_2$, the dynamics of the angular rate estimate can be decoupled from that of the asymmetric damping estimate. In this case, all estimates dynamics are decoupled, and therefore it is possible to adjust the dynamics of angular rate estimate independently, without significantly affecting the estimation dynamics of fabrication imperfections.

Applying the decoupling condition, the bandwidth of adaptive controlled gyroscope is approximately given by $BW \approx 2\gamma_\Omega X_0^2\omega_1^2$. Thus, the bandwidth of a MEMS gyroscope under observer based adaptive control is proportional to the adaptation gain γ_Ω and the energy of oscillation of the reference model.

5.2 Resolution Analysis

Measurement and Brownian noises limit the minimum detectable signal of angular rate estimate. The standard deviation of the angular rate estimate error, or resolution, is obtained from covariance matrix of trajectory estimation, trajectory and parameter estimation error dynamics of adaptive controlled gyroscope. Covariance $\boldsymbol{P_o}$ of $\boldsymbol{x_o}$ can be easily pre-computed independently of the mean trajectory by solving the following familiar Lyapunov equation.

$$\dot{\boldsymbol{P}}_o \approx \boldsymbol{P}_o\boldsymbol{A}_o^T + \boldsymbol{A}_o\boldsymbol{P}_o + \boldsymbol{G}_o\boldsymbol{S}_o\boldsymbol{G}_o^T \qquad (11)$$

where $\boldsymbol{x}_o = \left[e_p\ \dot{e}_p\ \tilde{q}_p\ \tilde{q}_v\ \tilde{\theta}\right]^T$, $\boldsymbol{S}_o = diag\ S_b, S_p$ and $\boldsymbol{A}_o, \boldsymbol{G}_o$ are corresponding error dynamics system matrixes. The ultimate achievable resolution can be calculated by setting $S_p = 0$ and computing $\boldsymbol{P}_o$ with equation (11). Simulation studies show that except for the small changes in the variance due to the control gain, only the angular rate adaptation gain γ_Ω significantly affects the variance. This implies that resolution can be adjusted by angular rate adaptation gain independently, without affecting other fabrication imperfection estimation dynamics, just as in the case of bandwidth.

5.3 Discussion

The main advantages of the adaptive mode of operation proposed in this paper include self-calibration, large robustness to parameter variations, and no zero-rate output. Moreover, because a single adaptive scheme controls all the operation tasks of the gyroscope, i.e. from initiating the vibratory motion of proof mass to estimating the angular rate, analytic predictions for the bandwidth and resolution of the gyroscope are easy to obtain and are relatively precise. The proposed adaptive controller design is also easy to implement in a high Q system. Thus, the noise properties associated with a high Q system can be fully utilized. Another advantage of the adaptive mode of operation is that it is easy to adjust the trade-off between bandwidth and resolution by simply adjusting the angular rate adaptation gain. In contrast, for a gyroscope operating under the conventional open-loop or force-balancing closed-loop mode of operation, the bandwidth and ultimate resolution of the gyroscope depend on the characteristics of the low-pass filter that is used to demodulate the angular rate estimate. Thus, it is difficult to adjust both the bandwidth and resolution, without changing the demodulation filter. Therefore, the adaptive mode of operation is better suited for medium-cost gyroscopes that are used in high-performance applications. One disadvantage of the adaptive mode of operation is that it cannot be applied to a conventional gyroscope structure. It should be noted that a conventional gyroscope structure is normally designed based on the assumption that the movement of the proof mass in the drive axis (say x-axis) is relatively large, but the movement in the sense axis (say y-axis) is very small. This means that for applying

proposed adaptive operation scheme of MEMS gyroscopes, a new gyroscope should be designed so that equal movement in the x and y axes is possible. Figure 2 shows a comparison between a conventional mode and an adaptive mode of operation. A detailed description of the design and fabrication process of new MEMS gyroscope is provided in [5].

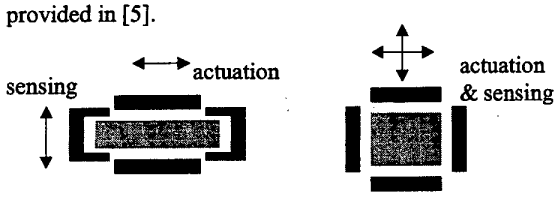

(a) conventional mode (b) adaptive mode

Figure 2. Comparison between a conventional and an adaptive mode

6 Simulation

A simulation study using the preliminary design data of the MIT-SOI MEMS gyroscope was conducted, to test the analytical results presented in this paper and verify its predicted performance. The data of some of the gyroscope parameters in the model is summarized in Table 1. For simulation purposes, we allowed ±5% parameter variations for the spring and damping coefficients and assumed ±1% magnitude in the nominal spring and damping coefficients for their off-diagonal terms. Notice that the simulation results are shown in non-dimensional units, which are non-dimensionalized based on the proof-mass, length of one micron and x-axis nominal natural frequency. The estimate of the angular rate response to a step input angular rate is shown in Figure 3. In this figure, the upper and lower bounds of its analytically estimated standard deviation are also plotted. These simulation results support the theoretical results obtained in this paper, and show that the realistic resolution of the adaptive controlled gyroscope is about 42 deg/sec/$Hz^{1/2}$, and the ultimate achievable resolution is about 0.70 deg/sec/$Hz^{1/2}$.

7 Conclusions

A new adaptive control approach for sensing angular velocity with a z-axis MEMS gyroscope was presented. The proposed control scheme can compensate manufacturing defects and is self-calibrating. The z-axis gyroscope under adaptive control has a large bandwidth, no ZRO and is robust to parameter variation. The proposed observer based adaptive control algorithm operates using only measurements of the x and y positions of proof mass of the MEMS z-axis gyroscope. The stability of observer based adaptive controlled gyroscope was rigorously proved. A complete convergence analysis shows that the dynamics of angular rate estimate can be decoupled from the dynamics of fabrication imperfection estimates, and bandwidth can be adjustable by adaptation gain if the energy of x and y axis dynamics of gyroscope is kept same. This analysis was verified with computer simulation.

Table 1. Key parameters of the gyroscope

parameter	*Value*
mass	$5.095x10^{-7}$ kg
x-axis frequency	*4.17* KHz
y-axis frequency	*5.11* KHz
Quality factor	10^4
Brownian noise PSD	$1.47x10^{-26}$ N^2sec
Position noise PSD	$1.49x10^{-27}$ m^2sec
Velocity noise PSD	$2.94x10^{-12}$ $(m/sec)^2$sec

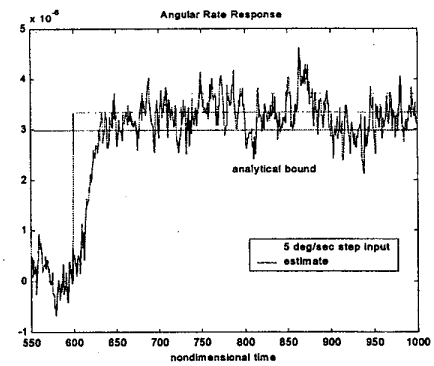

Figure 3. Time responses of angular rate estimate to 5 deg/sec step input

References

[1] Shkel, A., R.T. Howe and R. Horowitz, "Modeling and simulation of micromachined gyroscopes in the presence of imperfection", *Int. Conf. On Modelling and Simulation of Microsystems,* pp. 605-608, 1999.

[2] Clark, W.A., *Micromachined Vibratory Rate Gyroscopes*, Doctoral Thesis, U.C. Berkeley, 1997.

[3] Ljung, P.B., *Micromachined Gyroscope with Integrated Electronics*, Doctoral Thesis, U.C. Berkeley, 1997.

[4] Jiang, X., J. Seeger, M. Kraft and B.E. Boser, "A monolithic surface micromachined Z-axis gyroscope with digital output", *2000 Symposium on VLSI Circuits*, Honolulu, HI, USA, pp.16-19, June 2000.

[5] Park, S., *Adaptive Control Strategies for MEMS Gyroscopes*, Doctoral Thesis, U.C. Berkeley, 2000.

[6] Sastry, S. S., *Adaptive Control: Stability, Convergence and Robustness*, Prentice Hall, 1989.